

Numerical Analysis of the Behavior of Electromechanical Parameters of Asynchronous Motor with Universal Cage

Kalala Kalala¹, Lidinga Mobonda Flory², Messo Léonide⁴, Meni Babakidi Narcisse⁵, Bandekela Kazadi André⁶, Lilonga Boyenga Désiré⁷.

Abstract: In this article, we present the model of the universal cage asynchronous motor; like all other asynchronous motors by its constitution having two stators. The disturbed power supply, where the absence of the voltage of a phase of the electrical network does not offer the possibility of operating the cage motor by its three-phase stator. This is why the integration of a single-phase stator is the answer to this problem.

The objective of this article is to describe the behavior of the electromechanical parameters of the universal cage asynchronous motor by the two types of tests namely the no-load test and the load test on the two stators which are the three-phase stator and single phase stator.

A motor in which the two stators cannot operate simultaneously, the three-phase stator having priority and in the event of disturbance known as the absence of the voltage of one phase of the electrical supply network, the single-phase stator intervenes as a backup to ensure the continue motor operation without modifying these electromechanical parameters in terms of speed and power.

The mathematical equations based on the electromechanical quantities of the motor facilitate the evaluation of the performance of the universal cage asynchronous motor. These test models confirm that the rotational speed and the mechanical power of the motor are close in the two stators.

Keywords: Analysis, Numerical, Electromechanical Parameters, Asynchronous Cage Motor, Universal.

Date of Submission: 06-03-2023

Date of acceptance: 19-03-2023

I. INTRODUCTION

We present the technology of the design of the universal cage asynchronous motor combining two stators (three-phase and single-phase) which have only one squirrel-cage rotor for the rotational movement of the machine.

Cage asynchronous motors present the major areas of research towards which we wanted to orient ourselves in the design; then, this chapter will deal with the equations of the operating characteristics of the universal asynchronous motor, the equations on obtaining the stator windings of the asynchronous motor, the equations of the mechanical and electrical characteristics of the three-phase and single-phase stator, finally the different diagrams of the windings of the stator operating in single phase and that of the stator operating in three phase.

II. MODEL OF A MACU

II.2.1 Constitution

The universal asynchronous motor, like all other asynchronous motors due to its constitution and manufacturing materials, consists of two stator parts (two stators) in which we find the magnetic circuit, the winding or winding and a carcass. A squirrel-cage rotor with drive shaft or motor shaft.

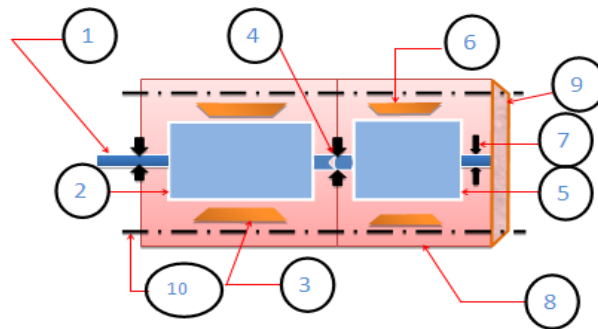


Figure II.1: Schematic diagram of MACU

Legend:

1. Motor or transmission shaft
2. Single-phase rotor
3. Single-phase winding
4. Landings
5. Three-phase rotor
6. Three-phase winding
7. rolling

II.2.2 Electrical equations

The choice of a representation model is made according to the type of command to be carried out. Thus, for a motor supplied with voltage, the components of the control vector of the state equation will be voltages. The electrical equations of the squirrel-cage asynchronous motor are those of the flux and voltage of the rotor and stator phases.

$$\begin{bmatrix} V_{Sa} \\ V_{Sb} \\ V_{Sc} \end{bmatrix} = \begin{bmatrix} R_s & 0 & 0 \\ 0 & R_s & 0 \\ 0 & 0 & R_s \end{bmatrix} \begin{bmatrix} i_{Sa} \\ i_{Sb} \\ i_{Sc} \end{bmatrix} + \frac{d}{dt} \begin{bmatrix} \phi_{Sa} \\ \phi_{Sb} \\ \phi_{Sc} \end{bmatrix} \quad (1.1)$$

$$\begin{bmatrix} 0 \\ 0 \\ 0 \end{bmatrix} = \begin{bmatrix} R_r & 0 & 0 \\ 0 & R_r & 0 \\ 0 & 0 & R_r \end{bmatrix} \begin{bmatrix} i_{r1} \\ i_{r2} \\ i_{r3} \end{bmatrix} + \frac{d}{dt} \begin{bmatrix} \phi_{ra} \\ \phi_{rb} \\ \phi_{rc} \end{bmatrix} \quad (1.2)$$

$$[\phi_{sabc}] = [L_{ss}][M_{sr}][i_{sabc}] \quad (1.3)$$

$$[\phi_{rabc}] = [L_{rr}][M_{rs}][i_{rabc}] \quad (1.4)$$

L_s and L_r respectively represent the stator and rotor inductance matrices, while M_{sr} and M_{rs} correspond respectively to the stator-rotor and rotor-stator mutual inductance matrices, their expressions are given by:

$$[M_{sr}] = [M_{rs}]^T = \begin{bmatrix} \cos\theta & \cos\left(\theta + \frac{2\pi}{3}\right) & \cos\left(\theta - \frac{2\pi}{3}\right) \\ \cos\left(\theta + \frac{2\pi}{3}\right) & \cos\theta & \cos\left(\theta + \frac{2\pi}{3}\right) \\ \cos\left(\theta + \frac{2\pi}{3}\right) & \cos\left(\theta - \frac{2\pi}{3}\right) & \cos\theta \end{bmatrix} \quad (1.5)$$

The matrix which establishes the relation between fluxes and currents in equation (I.3), contains mutual inductances M_{sr} and M_{rs} time-dependent, via the angle θ (rotor position). By replacing the equation (I.3) in the voltage equation (I.2), we obtain the equation which expresses the motor voltages as a function of the currents.

$$\begin{cases} v_{sabc} = [R_s][i_{sabc}] + \frac{d}{dt} ([L_{ss}][i_{sabc}] + [M_{rs}][i_{rabc}]) \\ v_{rabc} = [R_r][i_{rabc}] + \frac{d}{dt} ([M_{rs}][i_{sabc}] + [L_{rr}][i_{rabc}]) \end{cases} \quad (1.6)$$

II.2.3 Stator joule loss equations

We have the stator joule losses in a three-phase machine is obtained by the expression:

$$P_{js} = 3R \cdot I^2 \quad (1.7)$$

For a stable state, this loss is obtained by the following expression:

$$P_{jsst} = 3R \cdot I_{st}^2 \quad (1.8)$$

On the other hand, for an unstable regime, this loss will be obtained by the following expression:

$$P_{jsist} = 3R \cdot I_{ist}^2 \quad (1.9)$$

II.2.4 Variation of the resistance of the stator windings

We have the stator joule losses in a three-phase machine, for an unstable regime, this loss will be obtained by the following expression:

$$R_s = \frac{U}{I_{st}} \quad (1.10)$$

III. TEST ON THE THREE PHASE STATOR

III.1 No-load test

III.1.1 Stable current

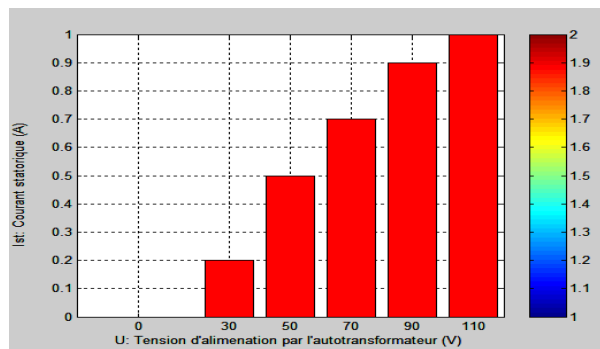


Figure III.1: MACU stator current measurement

The stable stator current of the three-phase stator, increases under the interval of 0A up to 1A for a no-load test.

III.1.2 Unstable current

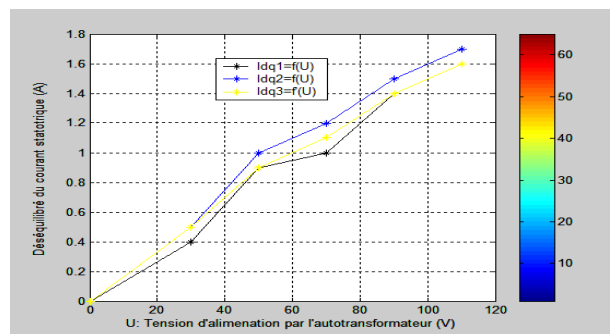


Figure III.2: Phase current unbalance

The simulation curves give the different points of the currents. The black curve describes the unstable current in the absence of phase 1 which increases under the interval of 0 A up to 6 A. The blue curve describes the unstable current in the absence of phase 2 which increases under the interval of 0 A up to 7 A. The yellow curve describes the unstable current in the absence of phase 3 which increases under the interval from 0 A up to 6 A. all these currents depend on the variation of the autotransformer voltage. This simulation is part of the no-load test.

III.1.3 Determination of Joule losses of three phases

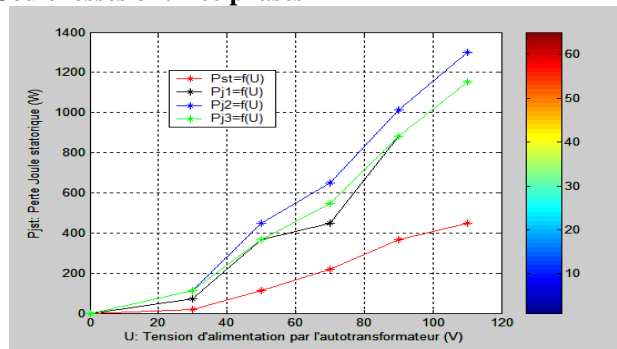


Figure III.3: Determination of Joule losses of three phases

The simulation curves give the different points of the stator losses of the asynchronous motor. The purple curve describes the behavior of the stator loss in unstable current which increases under the interval of 0 W up to 844.8 W. On the other hand the green curve describes the behavior of the stator loss in stable current which under the interval from 0 W up to 330 W. This simulation is part of the no-load test.

III.1.4 Determination of resistance on unbalanced currents

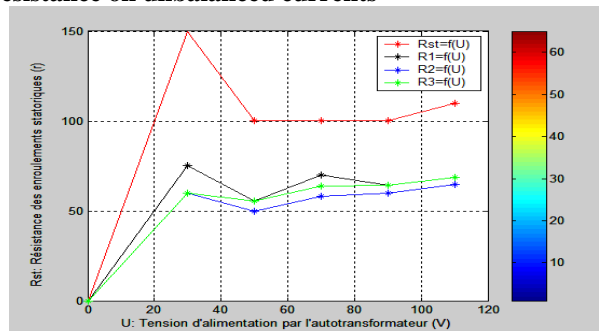


Figure III.3: Determination of resistance on unbalanced current 3

The simulation curves give the different points of the currents. The black curve describes the unstable current in the absence of phase 1 which increases under the interval of 0 A up to 4.4 A. The blue curve describes the unstable current in the absence of phase 2 which increases under the interval of 0 A up to 4.3 A. The yellow curve describes the unstable current in the absence of phase 3 which increases under the interval from 0 A up to 4.5 A. all these currents are a function of the variation of the supply voltage reduced from 0 V to 110 V. This simulation is part of the load test.

III.2 Load testing

III.2.1 Stable current under load

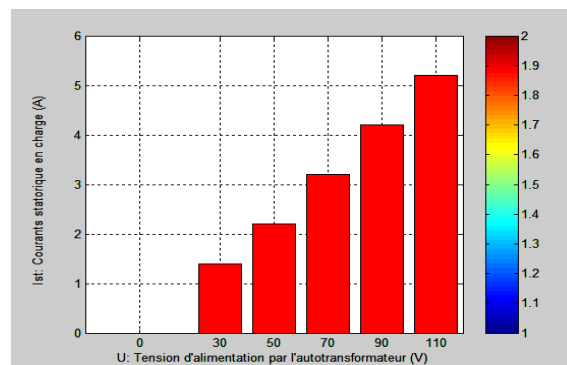


Figure III.4: Stable current under load

The stator current of the three-phase stator increases under the range of 0 A up to 5.2 A, for a load test.

III.2.2 Load current unbalance

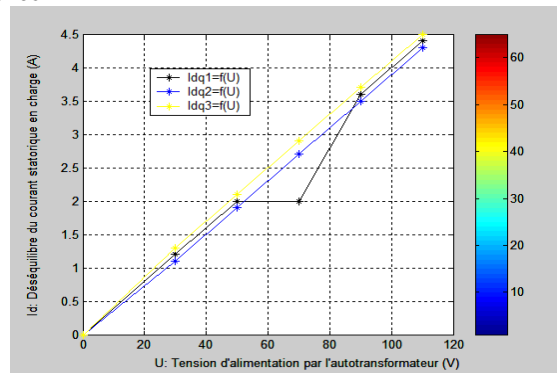


Figure III.5: Current unbalance on load of three phases.

The simulation curves give the different points of the currents. The purple curve describes the unstable current which increases under the interval of 0 A up to 4.5 A in the absence of phase T. The green curve describes the unstable current which increases under the interval of 0 A up to 4.3 A in the absence of the S phase. The red curve describes the unstable current which increases under the interval of 0 A up to 4.4 A in the absence of the R phase. The blue curve describes the stable current which increases under the range from 0 A up to 5.2 A. all of these currents are a function of the reduced supply voltage variation from 0 V to 110 V. This simulation is part of the load test.

III.2.3 Torque as a function of voltage

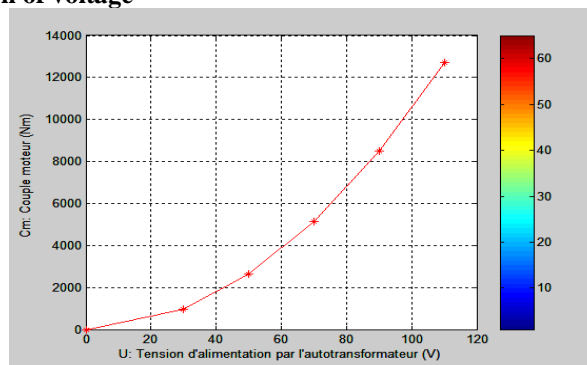


Figure III.6: Simulation of motor torque

The shape of the curve is almost rising, this curve describes the evolution of the motor torque as a function of the tension under the interval of 0 Nm up to 12100 Nm. This simulation is taken into account in the load test.

III.2.4 Torque as a function of absorbed current

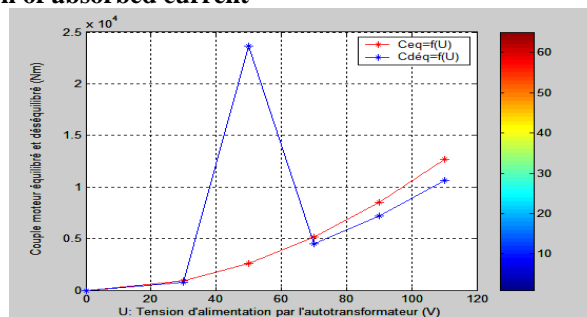


Figure III.7: Simulation of the different engine torques

The simulation curves give the different points of the motor torques. The blue curve describes the shape of the motor torque in the unstable current which increases under the interval of 0 Nm up to 10134 Nm. up to 12100 Nm.

IV. TEST ON THE SINGLE-PHASE STATOR

IV.1 No-load test

IV.1.1 Current measurement

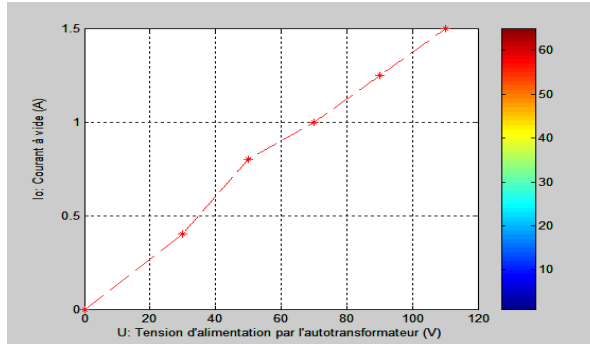


Figure IV.1: No-load phase current of the MACU

The simulation curve gives the different points of the no-load current of the single-phase stator. The current increases under the range of 0 A up to 1.5 A. This simulation is within the framework of the no-load test.

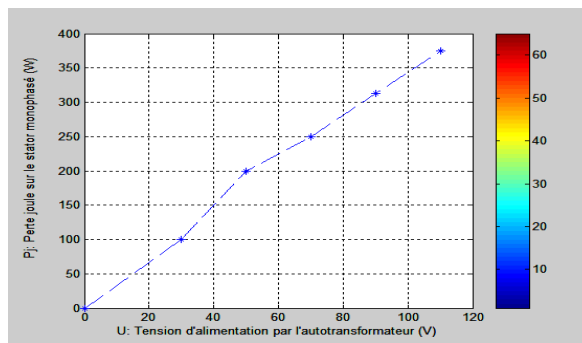


Figure IV.2: Joule loss determination

The simulation curve gives the different stator joule loss points of the single-phase stator. This increases under the interval from 0 W up to 375 W. This simulation is within the framework of the no-load test.

IV.1.3 Variation of single-phase stator winding resistance

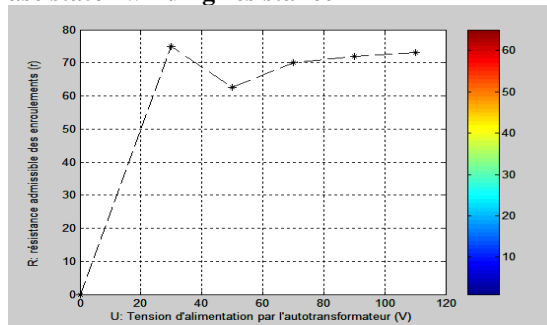


Figure IV.3: single-phase stator winding resistance

The simulation curve gives the different resistance points of the single-phase stator windings of the single-phase stator. This increases under the interval of 0Ω up to 73Ω. This simulation is part of the no-load test.

IV.2 Load testing Current measurement

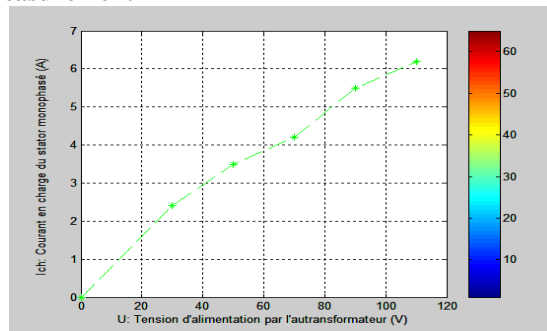


Figure IV.4: Measurement of the stator current on load of the MACU

The simulation curves give the different points of the current under load. The current increases under the range of 0 A up to 6.2 A. All these currents are a function of the variation of the voltage of the reduced power supply from 0 V to 110 V and within the framework of the load test .

V. CONCLUSION

In this article, we carried out the tests with load and load of the asynchronous motor within the laboratory of the tests of electric machines of the ISTA-Kinshasa, these tests made it possible to describe the behavior of the asynchronous motor with simple universal cage of the point view electromechanical parameter such as the unstable and stable no-load current as a function of the autotransformer voltage including the various stator losses of the asynchronous motor as a function of the voltage and the currents. This article to present calculation models allowing to describe the behavior of the universal cage asynchronous motor from the point of view of the following electromechanical parameter, the motor torque as a function of the voltage including the motor torque as a function of the stable and unstable current .

BIBLIOGRAPHY

- [1]. Abad, Lopez, Rodriguez, Marroyo, Iwanski, 2011. Doubly Fed Induction Machine: Modeling and control for wind energy generation. IEEE Press.
- [2]. Pouloujadoff, F, 1988. Graphical representation of doubly fed induction machine operation, electric machines and power systems. Electric Machines and Power Systems 15, 1988, pages 93 - 108.
- [3]. D. Aguglia , R. Wamkeue , P. Viarouge , J. Cros , "Exploring Suitable Applications for Doubly-Fed Asynchronous Machines". ICEMS conference 2008.
- [4]. HARKATI Nacereddine, HAUD Lachen, "Determination of the parameters of the asynchronous machine taking into account thermal, film and saturation effects". PFE in Electrotechnics, ENP of Algiers, year 2009.
- [5]. Joseph P. BORELLI, Richard BURKHART. New phase sensitive technology for capacitor-start motor simplifies application IEEE Transactions on Industry Applications, vol 34 – n°2, March – April 1998
- [6]. Jean-Pierre CARON, Jean-Paul HAUTIER Modeling and control of the asynchronous machine. Technip Editions, 1995, ISBN 2-7108-0683-5 – p.13-28, p.76-82
- [7]. G. CLERC, M. BESSAOU, P. SIARRY, P. BASTIANI. Identification of synchronous machines by genetic algorithm. RIGE Review, Volume 5 - No. 3-4/2002, p. 485-515, 2002
- [8]. Luc LORON. Parametric identification of the asynchronous machine by extended Kalman filter International Journal of Electrical Engineering, AC 3, n°2 – p. 163-205, 2000
- [9]. Hamid MB METWALLY New method for speed control of single-phase induction motor with improved motor Performance. Energy Conversion & Management, vol 42, 2001. Elsevier Science Ltd, Pergamon Press
- [10]. Frédéric FERREYRE, René GOYET, Guy CLERC, Thierry BOUSCASSE Sensorless slowdown detection method for single-phase induction motors. IEEE Transactions on Energy Conversion, vol. 24, n°1, March 2009 – p. 60-67.

BIBLIOGRAPHY



Kalala Kalala . Diploma from Master's degree 2017 University of Brazzaville-Congo and PhD student in engineering sciences of The University of Brazzaville-Congo.
Assistant-Teacher at ISTA-



Prof. Dr. Ir Lidinga Mobonda Flory ,
PhD In Engineering Sciences, Dept. Of
Electricity.
ENSP-UMNG Electrical Engineering
Research Laboratory
Teacher-Researcher at ISTA-Boma



MA. Dr. Ir , Leonide Messo . PhD In
Engineering Sciences, Dept. Of
Electricity.
ENSP-UMNG Electrical Engineering
Research Laboratory
Teacher-Researcher at ENSP



Prof. Dr. Ir Narcisse MeniBabaka,
Ph.D,
Universidad Michoacana de San
Nicolás de Hidalgo (UMSNH)
Mexique.2017-2021,
Teacher-Researcher at ISTA-Kinshasa



Prof. Dr. Ir André Bandekela Kazadi ,
is an electrical engineer, he received
his PhD, from the energetic institute of
Moecou (Rusie). Director of the ISTA-
Kin doctoral school



Prof. Dr Desire LILONGA BOENGA
presently lecturer at the
University of Brazzaville-Congo, Dept.
Electronics
Teacher-Researcher at ENSP